SEISMIC DEFORMATIONS OF DIFFERENT SIZE EMBANKMENTS ON A SPATIALLY VARIABLE LIQUEFIABLE DEPOSIT

Nicholas A. Paull¹ Ross W. Boulanger² Jason T. DeJong³

ABSTRACT

Evaluating the potential for seismic deformation of an embankment on a liquefiable deposit requires consideration of the deposit's spatial variability, the scale of any potential deformation mechanisms, and the quality of the site characterization information, among other factors. Seismic evaluations of embankment dams and levees using finite difference or finite element analyses commonly represent strata with equivalent representative uniform properties, rather than explicitly modeling the spatial variability. The present study examines different size embankments on a spatially variable (stochastic) liquefiable alluvial deposit to determine the effect of embankment size on the potential variability in seismic deformations and the selection of equivalent representative uniform properties. The nonlinear deformation analyses are performed using the finite difference software FLAC 8.0 with the user-defined constitutive model PM4Sand for the liquefiable soils. The four embankments analyzed vary from 5 m to 45 m high, and the foundation layer is modeled with both uniform soil properties and stochastic distributions of soil properties generated by a geostatistical model. A set of ground motions with a range of characteristics scaled to different peak ground accelerations is used. The results enable evaluation of how the scale of the embankment (and its associated deformation mechanisms) relative to the scales of fluctuation in the liquefiable layer affect the variability in predicted deformation and how equivalent representative uniform soil properties should be selected for use in uniform analysis models.

INTRODUCTION

Nonlinear deformation analyses (NDAs) are commonly used to assess the expected deformations of embankment dams and levees that are subjected to earthquake loading. Knowledge of the local geology along with site explorations (borings, lab tests, etc.) are used to assess input properties for NDAs. Seismic analyses of the embankments are then performed using several different motions (consistent with the seismic hazard) on NDA models with generally uniform properties (called uniform models) intended to produce reasonable system-level responses. These uniform models do not explicitly take into account spatial variability of the soil but rather use "representative" percentile properties to indirectly account for the spatial variability.

1

¹ Graduate Student, Department of Civil & Environmental Engineering, University of California, Davis, CA 95616, napaull@ucdavis.edu.

² Professor, Department of Civil & Environmental Engineering, University of California, Davis, CA 95616, rwboulanger@ucdavis.edu.

³ Professor, Department of Civil & Environmental Engineering, University of California, Davis, CA 95616, jdejong@ucdavis.edu.

The selection of representative percentile properties for use in uniform NDA models is usually guided by past practice and engineering judgment, recognizing that selected values depend on the purpose of the analyses; e.g., a representative property could be intended to provide an unbiased (best) estimate versus a conservative estimate of a specific type of damage (e.g., crest settlement, racking of an embedded structure, deformation of foundation drains). For example, one common practice for embankment dams has been to use 33rd percentile Standard Penetration Test (SPT) or cone penetration test (CPT) penetration resistances for determining the properties of individual liquefiable strata (e.g., Perlea and Beaty 2010), which is generally consistent with studies showing that the use of mean or median properties for a liquefiable stratum can significantly underestimate earthquake-induced excess pore pressures or deformations (e.g., Popescu et al. 1997, Boulanger and Montgomery 2016). Insights on the selection of representative properties in spatially variable deposits can also be obtained from the numerous studies for other types of problems and structures, wherein the selection has been shown to depend on the nature of the structure, the scales of any deformation mechanism, the scales of fluctuation in soil properties, and the desired degree of conservatism (e.g., Baecher and Christian 2003, Fenton and Griffiths 2005).

This paper examines the selection of representative properties for use in NDAs of embankment dams of different sizes founded on a liquefiable alluvial stratum. The selection of representative properties for different geologic and site investigation scenarios are first discussed within the framework of a hypothetical segment of an event tree for a risk analysis. The effect of embankment size on selection of representative properties for an alluvial foundation layer is then examined for the event tree scenario where soil variability is assessed using site investigation data from adjacent sections. NDAs are performed for "uniform" models with uniform SPT (N₁)_{60cs} values assigned to the alluvial layer and "stochastic" models with unconditioned, spatially correlated, Gaussian random fields of SPT $(N_1)_{60cs}$ values assigned to the alluvial layer. The NDA results are used to determine the representative percentiles of the stochastic $(N_1)_{60cs}$ values that, when used in a uniform model, produce different measures of embankment deformation (e.g., crest settlement, shell displacements) equal to those from the stochastic (random field) models. The representative percentiles are shown to vary significantly with the size of the embankment relative to the scales of fluctuation used to describe the soil's spatial variability. The implications of these results for practice are discussed.

REPRESENTATIVE PROPERTIES FOR SEISMIC EVALUATION OF EMBANKMENTS

Development of Geologic Models

One of the initial steps for analysis of seismic deformations of an embankment is to evaluate the soil stratigraphy along the entire alignment and develop a geologic model based on the geologic formational history of the site. Confidence in the interpreted geologic model can vary, depending on the complexity of the site, the extent and quality of the site investigations, and whether the interpretation is preliminary or final.

Allowance should be made, as indicated by the first branch in the event tree segment shown in Figure 1, for the possibility that the interpreted geologic model may be significantly inaccurate due to insufficient understanding of the formational processes or because a significant geologic feature was missed in the site investigation, especially in cases where site investigation data are sparse. An inaccuracy in the geologic model would be considered significant if it could affect seismic deformations enough to influence the computed risk or final decisions. Hypothetical (alternative) geologic models can be developed that are consistent with the site geology and available data, such as including a looser buried channel or connecting a looser continuous layer, followed by an evaluation of whether such features are large/extensive enough to impact the structure being evaluated. Explicitly allowing for the possibility that the interpreted geologic model may be inaccurate and that alternative geologic models may be applicable provides the basis for evaluating the potential benefits of performing more intensive site investigations to increase confidence in the interpreted geologic model.

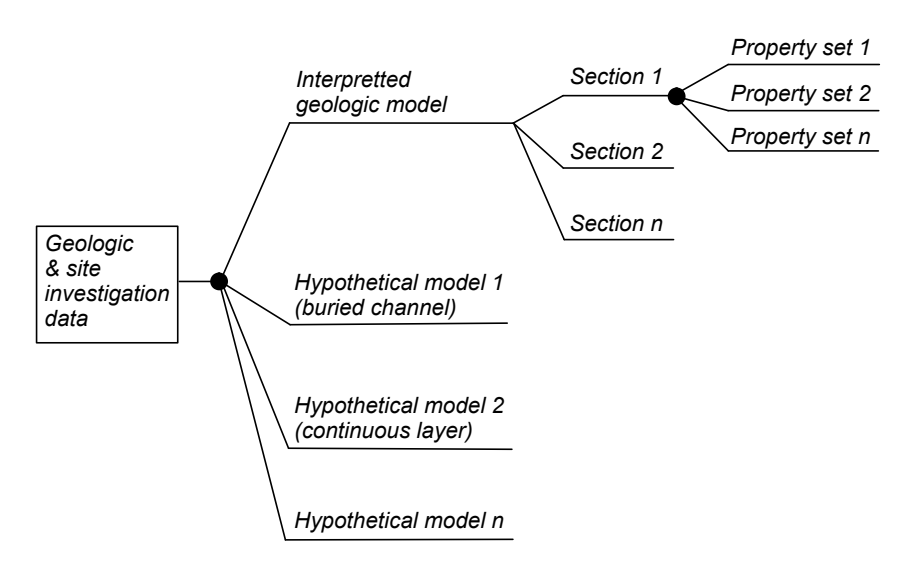


Figure 1. Event tree segment for seismic risk evaluation.

Representing Spatial Variability

The geologic models (interpreted or hypothetical) can then be used to generate the analysis cross-sections for the NDAs (second branch in Figure 1). The analysis cross-sections need to represent all possible reaches (i.e., segments of the embankment length) over which significant deformations could develop largely independent of the adjacent reaches. The minimum reach length therefore depends on the scale of the potential deformation mechanisms, which depends on the size of the embankment.

Properties can then be assigned to individual strata in the analysis cross-sections, using different approaches to account for the potential effects of spatial variability (third branch in Figure 1). For NDAs that use the interpreted geologic model, one approach would be to explicitly model the spatial variability of soil properties using either unconditioned or conditioned random fields. For cross-sections representing reaches within which SPT or CPT data are available, the random fields can be conditioned on those data. For cross-

sections representing reaches within which SPT and CPT data are not available, the random fields must be generated based on data elsewhere in the same geologic unit. Therefore, a greater frequency of site explorations along the embankment length increases the portion of the embankment length that can be analyzed using conditioned random fields, which would be expected to reduce uncertainty relative to the use of unconditioned random fields. In either case, a number of stochastic realizations would then be generated for each stratum (i.e., the property sets branch in Figure 1) to explicitly incorporate spatial variability into the NDA models.

A second approach to account for the effects of spatial variability would be to use uniform NDA models with a distribution for the representative properties used to represent any given stratum. The distribution of representative properties would be selected to produce a distribution of embankment deformations that would be expected to approximate the distribution that would have been obtained with stochastic models. This approach might use a simple three-point distribution for the representative properties, thereby requiring fewer NDA simulations compared to the use of stochastic models. The remainder of this paper examines the selection of representative values for this approach for cases where the stochastic properties would otherwise be represented with unconditional random fields.

Prior Studies on Selecting Representative Percentiles for Liquefiable Deposits

NDAs with stochastic realizations have been used to study liquefaction effects for level ground (Popescu et al. 1997, 2005), gently sloped ground (Montgomery and Boulanger 2017), and embankment dams (Boulanger and Montgomery 2016). Popescu et al. (1997, 2005) performed 2D and 3D analyses of level ground and suggested that the 20th percentile was generally conservative for obtaining estimates of maximum excess pore pressure ratio (r_{u max}). Montgomery and Boulanger (2017) completed 2D NDAs with gently sloped ground and concluded that representative percentiles for predicting the expected value of lateral spreading displacements generally ranged from the 30th to 70th percentile. Boulanger and Montgomery (2016) completed 2D NDAs of a 45 m high embankment on an alluvial foundation and concluded that representative percentiles for predicting expected values for the crest settlement or shell displacement generally ranged from the 33rd to 50th percentile. These latter two studies showed that representative percentiles for the liquefiable layer decreased as the thickness of the layer increased, the relative density of the soil decreased, the overburden stress increased, the ground slope increased, and the shaking intensity decreased (or magnitude of deformation decreased). In addition, a wider range of representative percentiles was required to approximate the distribution of ground displacements obtained with the stochastic models for the lateral spreading problem than for the 45 m high embankment problem.

NDA EMBANKMENT MODEL

Model Configuration

Four different size embankments, shown in Figure 2, were analyzed using the 2D finite difference program FLAC 8.0 (Itasca 2016). Each analysis model had four material

groups; the bedrock layer, the alluvial layer, the center clay core, and the embankment shells. All embankment slopes were 2.5:1 (H:V) except for the lower portion of the downstream slope which was 3.5:1. All models had a 6 m wide crest, a 15 m thick bedrock layer, and a 12 m thick alluvium layer. Models were 400 m wide to ensure that the lateral boundaries did not significantly affect the deformation results. Soil elements (or zones) were generally about 0.25 m high in all models to ensure that all frequency components of interest can be appropriately transmitted.

Each embankment was incrementally built in horizontal layers to simulate the construction process and provide realistic initial stress conditions. Once the embankment construction is complete, the reservoir water level was raised in five steps. The final reservoir level was at 75% of the embankment height. The vertical and horizontal stresses, coefficient of earth pressure at rest (K_0), initial static shear stress ratio (α) and other factors were checked to ensure that the initial static stress and seepage conditions were reasonable and within expected ranges (Boulanger and Beaty 2016).

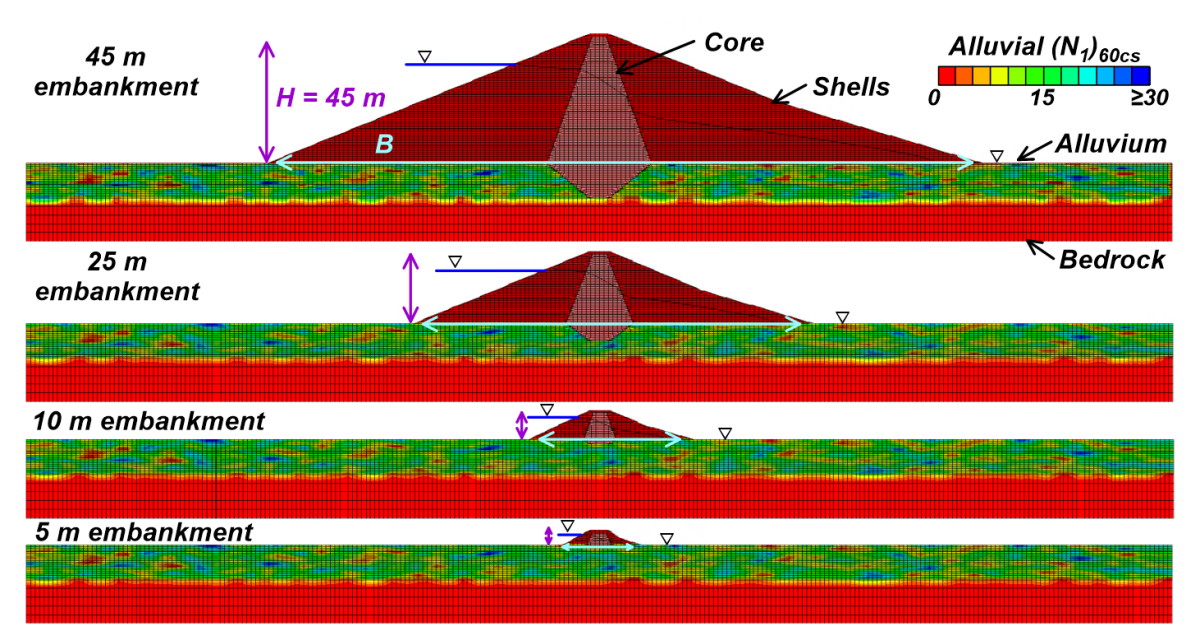


Figure 2. Embankment model geometries with the same realization of $(N_1)_{60cs}$ in the alluvium group.

Material Properties and Model Calibration

The bedrock was modeled as an elastic material with shear modulus G=1800 MPa, Poisson's ratio ν =0.3, and saturated unit weight, ρ =2.2 Mg/m³, which together correspond to a shear wave velocity V_s =900 m/s. The bedrock permeability was 5.0E-6 cm/s.

The clay core was modeled as a Mohr-Coulomb material with undrained shear strengths for the dynamic loading phase based on the initial static consolidation stresses prior to dynamic loading. The undrained shear strengths were computed using the procedures in Duncan and Wright (2005) as applied to NDA models by Montgomery et al. (2014). The undrained shear strength parameters for isotropic consolidation were d_R =33 kPa and

 ψ_R =14°, and the drained shear strength parameters were d_S (or c')=0 and ψ_R (or ϕ ')=36°. The shear modulus was set proportional to the square root of the mean effective stress (p'), with G= 43 MPa at p'=101.3 kPa. The permeability was 5.0E-5 cm/s and the saturated unit weight was ρ =2.0 Mg/m³.

The shells were modeled using PM4Sand version 3.1 (Boulanger and Ziotopoulou 2018) with properties based on a uniform SPT $(N_1)_{60cs}$ = 35 for the entire group. The relative density (D_R) and shear modulus coefficient (G_o) were set to 87% and 1022, respectively, based on the correlations used in Boulanger and Ziotopoulou (2018). The contraction rate parameter (h_{po}) was calibrated based on single-element direct simple shear simulations to match the cyclic resistance ratio (CRR) based on the SPT based liquefaction triggering correlation from Boulanger and Idriss (2012). The remaining PM4Sand input parameters were kept at the default values. The permeability was 5.0E-4 cm/s and the saturated unit weight was ρ =2.1 Mg/m³.

The alluvium group was modeled using PM4Sand version 3.1 with the properties for each individual zone based on its assigned SPT $(N_1)_{60cs}$ value. SPT $(N_1)_{60cs}$ values were input as uniform values or as Gaussian random fields as described in the next section. The D_R , G_o and h_{po} were based on the same correlations and procedure described for the shells. The remaining PM4Sand input parameters were kept at their default values. The permeability was 5.0E-4 cm/s and the uniform unit weight was ρ =2.0 Mg/m.

Stochastic Realizations of the Alluvial Group

The alluvium is the only material that is represented by stochastic realizations. The alluvial group has properties that are correlated to SPT blow count, $(N_1)_{60cs}$, and are represented in uniform models by a single $(N_1)_{60cs}$ value and in the stochastic models by spatially correlated, Gaussian random fields of $(N_1)_{60cs}$. The $(N_1)_{60cs}$ values were truncated so that there were no negative values, with the truncation affecting less than 0.5% of the elements.

A set of seven stochastic realizations of $(N_1)_{60cs}$ were generated based on unconditioned, spatially correlated, Gaussian random fields. All realizations have a mean $(N_1)_{60cs}$ of 15 and a coefficient of variation (COV) of 40%. The cumulative distributions for the seven realizations are presented in Figure 3. Scales of fluctuation (θ) are used to control the spatial structure of the Gaussian random fields and are defined as a measure of distance within which points are significantly correlated (Vanmarcke 2010). The anisotropic scales of fluctuation are assigned with a value in the horizontal direction (θ_x) of 20 m and a value in the vertical direction (θ_y) of 1 m. The ratio of these scales of fluctuation is consistent with Phoon and Kulhawy (1999) who observed that they are typically at least an order of magnitude different. NDA results are later discussed in terms of the normalized scale of fluctuation in the horizontal direction (NSF_x= θ_x /B) where B is the base length of the embankment in the cross-sectional direction.

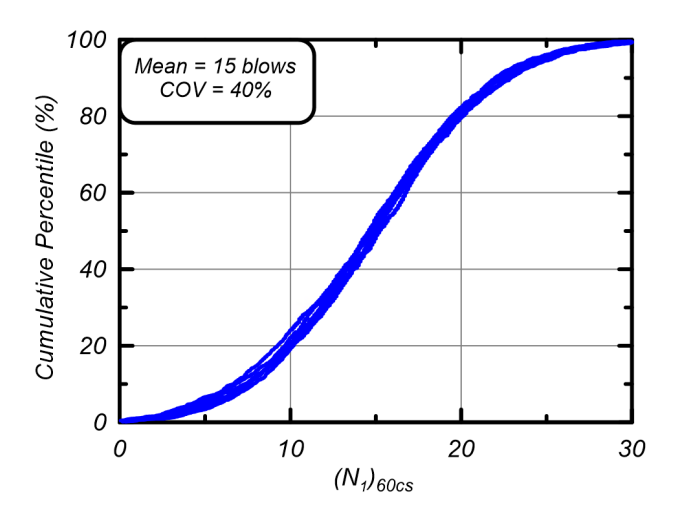


Figure 3. Cumulative distributions of $(N_1)_{60cs}$ for seven unconditioned, spatially correlated, Gaussian random field realizations for the alluvium group.

Input Motions

All embankment models (uniform and stochastic) were subjected to three input motions, each scaled to three peak ground accelerations (PGAs) between 0.2 g and 0.8 g. The input motions, obtained from the NGA-West2 database (Ancheta et al. 2014), are the Mudurnu station fault normal (FN) motion from the 1999 Duzce earthquake (M=7.1), the TCU075 station east-west recording from the 1999 Chi-Chi earthquake (M=7.6) and the TAPS pump station number 10-047 recording from the 2002 Denali earthquake (M=7.9). These motions (see Figure 4) were chosen to represent a variety of spectral shapes and ground motion characteristics so that the findings can be applicable for a wide variety of ground motion loading scenarios.

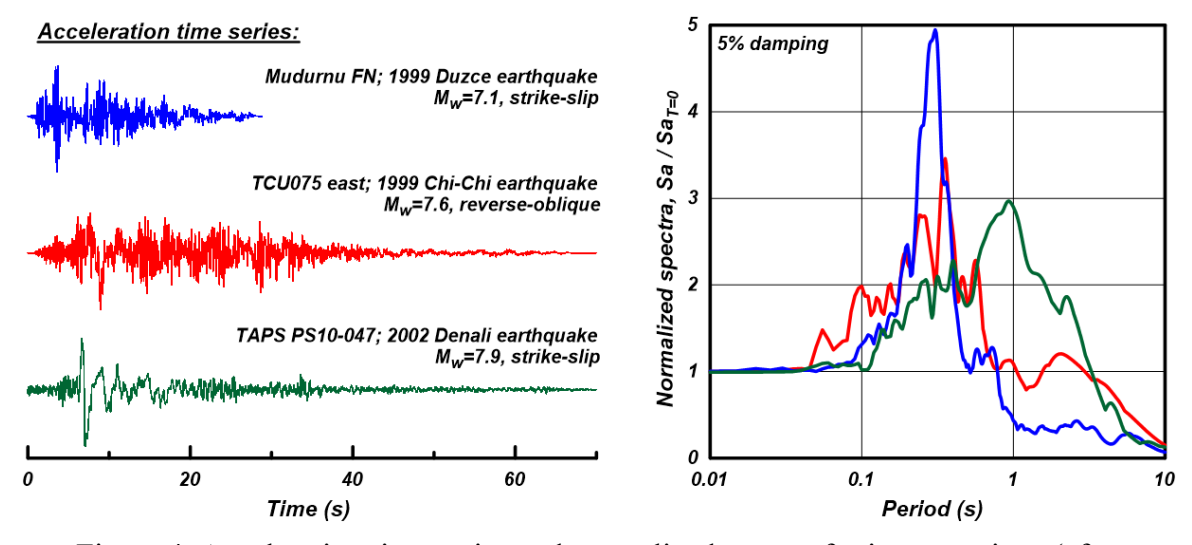


Figure 4. Acceleration time series and normalized spectra for input motions (after Boulanger and Montgomery 2016).

Outcrop motions were applied as a shear stress time series to the compliant base of the embankment models (Mejia and Dawson 2006). Free field conditions were applied at the lateral edges of the models, with the outer column of elements on each edge of the alluvium replaced with an equivalent elastic material to maintain confinement on the PM4Sand elements. All materials were damped using Rayleigh damping of 0.5% at a frequency of 3 Hz to provide a minimum level of damping in the small strain range for the nonlinear materials and a nominal damping for the linear elastic bedrock material.

MODEL RESULTS

Deformation Analyses

Displacements for the uniform and stochastic embankment models are compared herein using the vertical crest settlement, horizontal displacements of the embankment toes and horizontal displacement of a point directly below the crest at the height of the top of the free field alluvium obtained at the end of shaking. The embankment "stretch," defined as the sum of the outward horizontal displacements at the embankment toes, and embankment "translation", defined as the horizontal displacement of a point directly below the crest and at a height even with the of the top of the free field alluvium, were found to be useful measures for comparing results across different models and motions. The displacements obtained from stochastic models were compared to the displacements obtained from uniform models to obtain representative percentiles for crest settlement (P_{set}), embankment stretch (P_{str}), and embankment translation (P_{trans}). Representative percentiles for this study are the cumulative percentile of the (N_1)60cs data that when input as a uniform property, produces the same displacement as a stochastic model.

Normalized crest settlements and the corresponding representative percentiles (P_{set}) for the 45 m and the 10 m high embankments are shown in Figures 5a and 5b, respectively. Uniform models had $(N_1)_{60cs}$ values of 7.5, 10, 12.5, 15, 17.5 and 20 which when compared to the cumulative distribution of (N₁)_{60cs} correspond to the 10th, 20th, 34th, 50th, 66th and 80th percentiles. The normalized crest settlements, shown in the upper plots, increase with increasing PGA and decreasing embankment size. A representative percentile for each stochastic realization is linearly interpolated from the uniform model results. The interpolated representative percentiles are shown on the lower plots of Figure 5. Values that fall below the 10th percentile are plotted at the 5th percentile and values that fall above the 80th percentile are plotted at the 90th percentile because these values are not well defined by the limited number of realizations and the ranges covered by the uniform models. The normalized crest settlement and corresponding representative percentiles for the 10 m high embankment have greater dispersion than for the 45 m high embankment. Representative percentiles range from the 42nd-55th for the 45 m embankment and from the 25th-75th for the 10 m embankment for embankments subjected to the TAPS PS10-047 motion as shown in Figure 5.

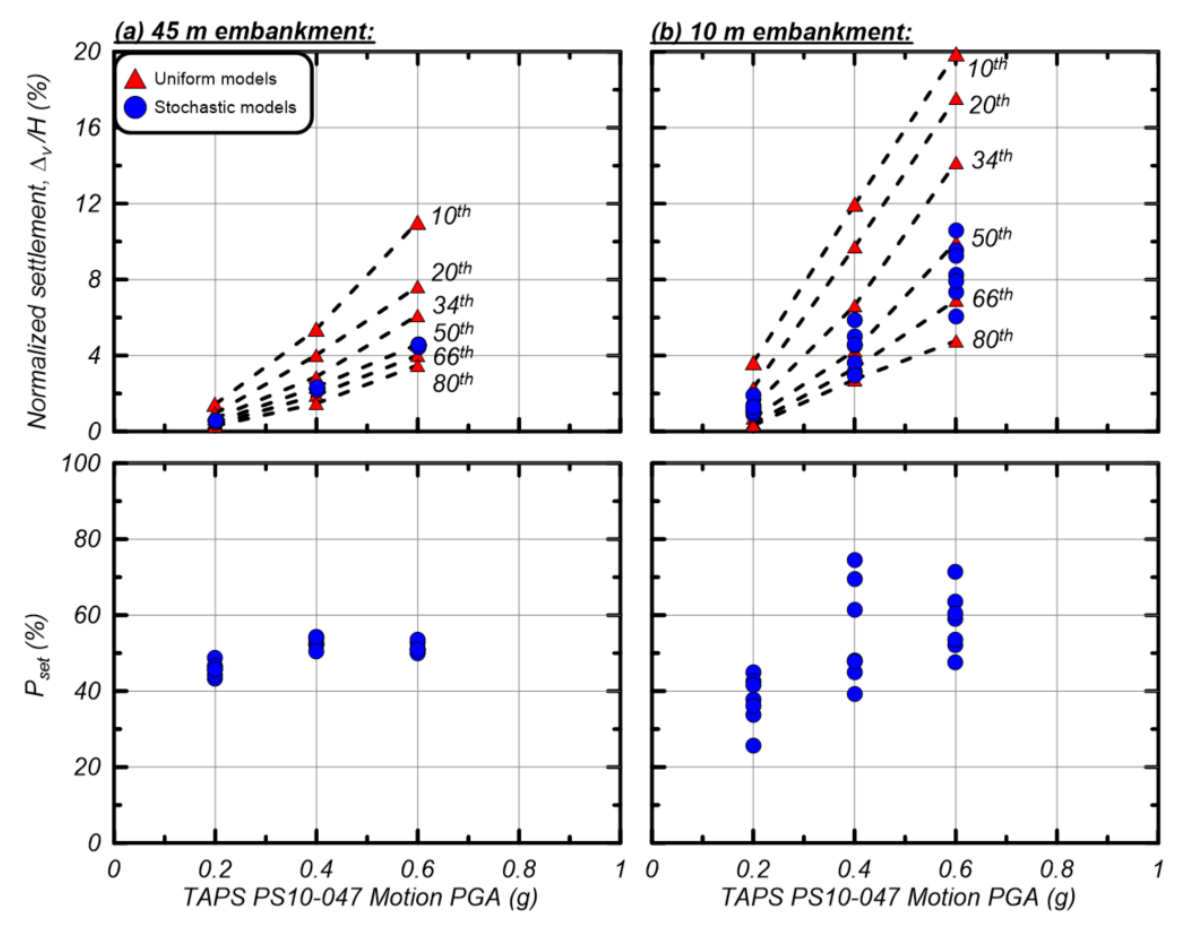


Figure 5. Normalized crest settlements and P_{set} for the TAPS PS10-047 motion: (a) 45 m high embankment, and (b) 10 m high embankment.

Effect of Embankment Scale

Large embankment models can have deformation mechanisms that engage a larger volume of soil than smaller embankment models. This is illustrated in Figures 6 and 7 showing results for a 45 m and 10 m high embankment with the same stochastic realization for the alluvium (Figures 6a and 7a) and same input motion. The deformation mechanisms are visible in the contours of maximum shear strain (Figures 6b and 7b), showing that the larger embankment causes a much larger soil volume to develop large strains. Therefore, for the 45 m high embankment dam, the deformation behavior is dependent on the properties of a much larger soil volume than for the 10 m high embankment, which results in greater averaging of soil resistances and less dispersion in predicted deformations as shown previously in Figure 5.

Small embankment models can have deformation mechanisms that engage a smaller volume of soil than large embankment models and can vary significantly from one realization to another. This is illustrated in Figures 7 and 8 for a 10 m high embankment with different stochastic realizations for the alluvium subjected to the same input motion. The stochastic realization in Figure 7a, which has no significantly stronger zones along the base of the embankment, developed a relatively large crest settlement ($P_{\text{set}} = 23\%$)

and relatively large downstream toe movement (resulting in P_{str} 18%), but a relatively small average downstream translation (resulting in $P_{trans} > 80\%$). The stochastic realization in Figure 8a which has a stronger shallow zone beneath the downstream shell, developed a relatively small crest settlement ($P_{set} > 80\%$) and relatively small embankment stretch ($P_{str} > 80\%$), but a relatively large average downstream translation due to a deeper deformation mechanism ($P_{trans} = 37\%$). These results show that deformations of smaller embankments can be controlled by localized zones of stronger or weaker soil, which can produce a larger dispersion in representative percentiles and a greater variation in representative percentiles between different displacement measures.

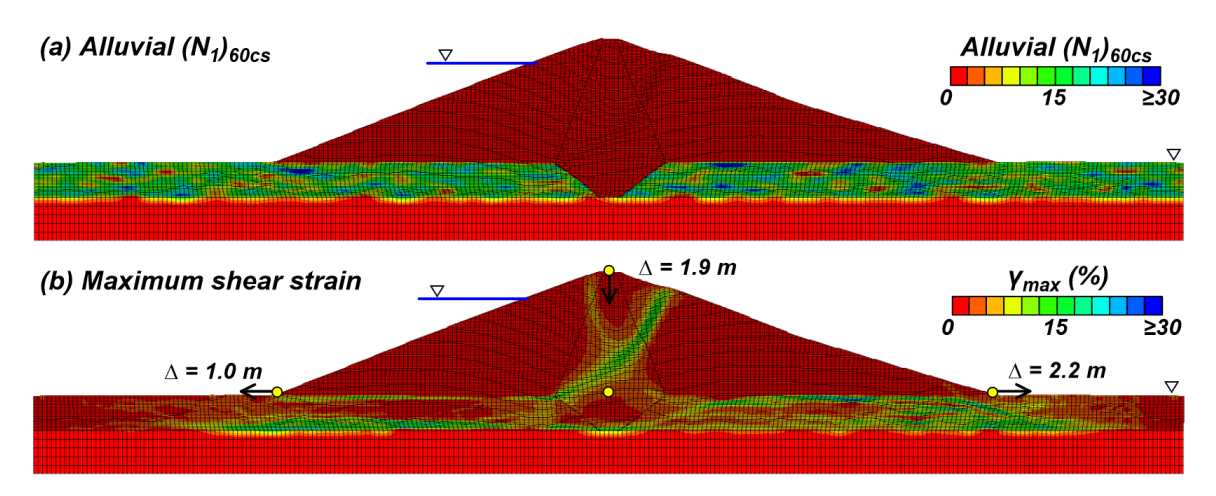


Figure 6. The 45 m embankment stochastic model subjected to the Mudurnu motion with a PGA of 0.8 g, $P_{set} = 52\%$, $P_{str} = 60\%$ and $P_{trans} = 52\%$.

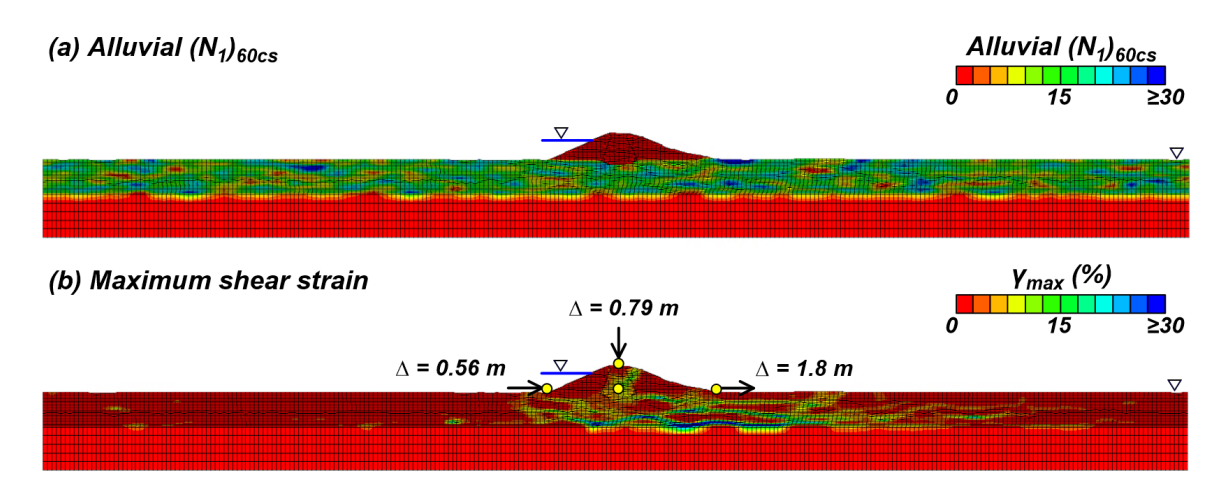


Figure 7. The 10 m embankment stochastic model subjected to the Mudurnu motion with a PGA of 0.8 g, $P_{set} = 23\%$, $P_{str} 18\%$ and $P_{trans} > 80\%$.

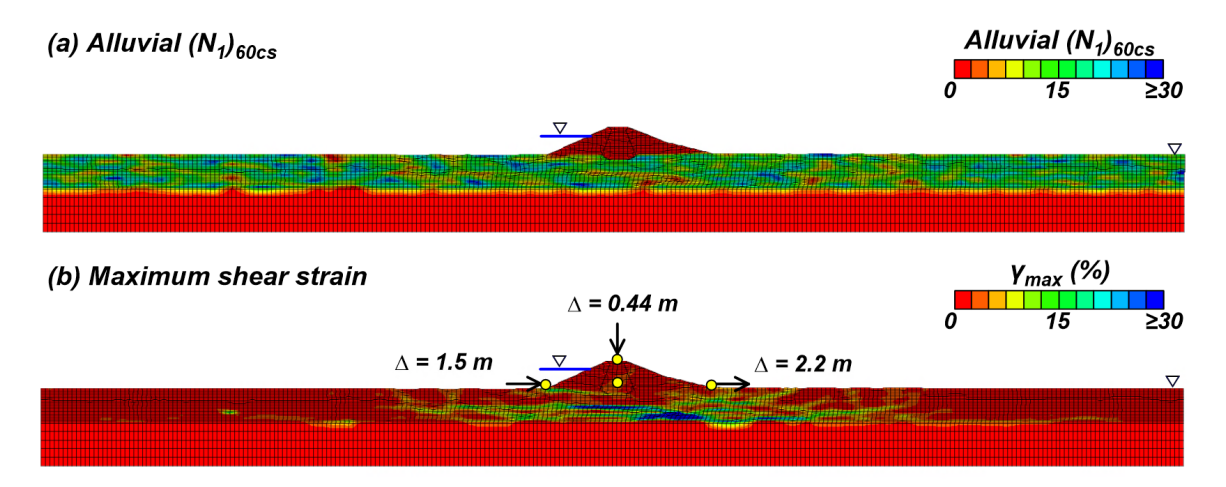


Figure 8. The 10 m embankment stochastic model subjected to the Mudurnu motion with a PGA of 0.8 g, $P_{set} > 80\%$, $P_{str} > 80\%$ and $P_{trans} = 37\%$.

The effect of embankment size on representative percentiles is illustrated in Figure 9 showing representative percentiles for the different embankments subjected to the same TAPS PS10-047 motion at a PGA of 0.6 g. Representative percentiles based on crest settlement (Figure 9a) and embankment stretch (Figure 9b) are plotted versus the normalized horizontal scale of fluctuation (NSF_x = θ_x /B). Since the horizontal scale of fluctuation for these realizations is a constant (20 m), the NSF_x only changes based on the embankment base width (B). The embankment with the smallest NSF_x (the 45 m high embankment) produced the smallest ranges in representative percentiles with P_{set} = 50^{th} - 54^{th} , P_{str} = 49^{th} - 59^{th} and P_{trans}= 46^{th} - 49^{th} for the TAPS PS10-047 motion at a PGA of 0.6 g. Increasing the NSF_x (decreasing the embankment size) increases the dispersion (range) of the representative percentiles and produces cases outside the 10^{th} and 80^{th} percentile limits examined by the uniform models. The median representative percentiles ranges from the 37^{th} to 60^{th} percentile for all modeled embankments subjected to the TAPS PS10-047 motion at a PGA of 0.6 g.

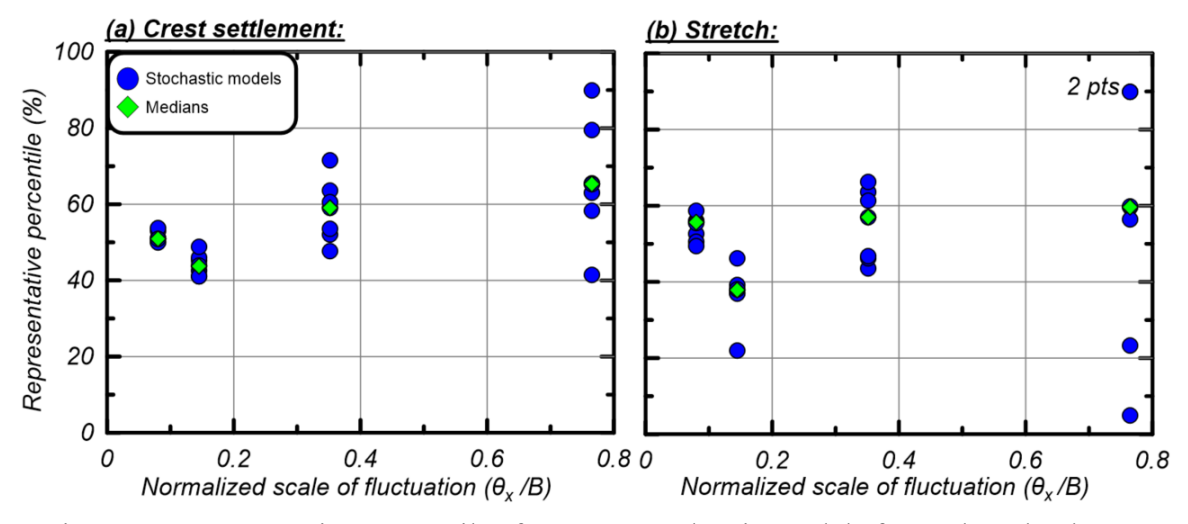


Figure 9. Representative percentiles for seven stochastic models for each embankment subjected to the TAPS PS10-047 motion at a PGA of 0.6 g (total of 28 cases).

The effect of input motion on representative percentiles is illustrated in Figure 10 showing representative percentiles based on crest settlement (Figure 10a) and embankment stretch (Figure 10b) versus NSF_x for all embankment models and input motions. The 45 m high embankment (smallest NSF_x) produces the smallest ranges of representative percentiles with P_{set} = 43th-58th, P_{str} =44th-66th and P_{trans}= 43th-55th. These results are generally consistent with the representative percentiles from Boulanger and Montgomery (2016) for the same height of embankment. For the 5 m and 10 m high embankments (largest NSF_x), several representative percentiles fall outside the 10th and 80th percentiles for both crest settlement and embankment stretch. The ranges in these representative percentiles (Figure 10) are larger than obtained for individual motions and PGAs (e.g., Figure 9), indicating that uncertainty in ground motion characteristics can contribute to uncertainty in the representative percentiles. The median representative percentiles range the 41st-58th percentile with no obvious dependency on NSF_x.

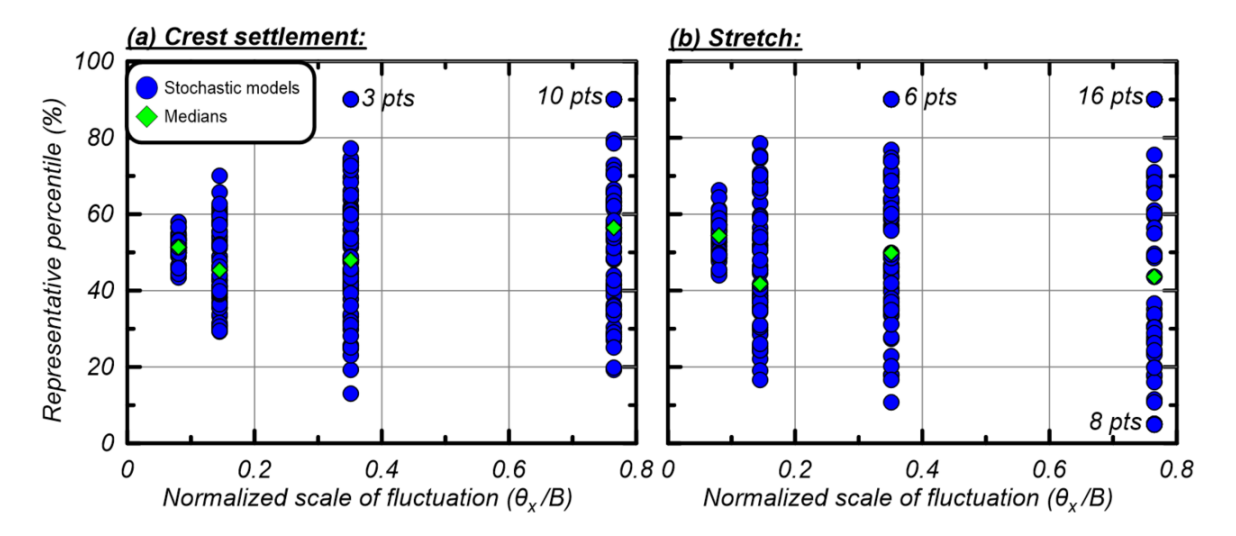


Figure 10. Representative percentiles for seven stochastic models of embankments of different sizes subjected to all motions and PGAs (total of 252 cases).

The dispersion or range in representative percentiles tend to be greater for embankment stretch (Figures 9b and 10b) than for crest settlement (Figure 9a and 10a). This trend suggests that horizontal movement of the embankment toes may be more difficult to predict than crest settlements. This trend is attributed to the fact that localized deformation at an embankment toe can develop in a smaller volume of soil, which results in less averaging of soil behaviors. In addition, the representative percentiles for crest settlement, embankment stretch, and embankment translation were only loosely correlated, such that high values for P_{set} sometimes coincide with smaller values for P_{str} or P_{trans}. Uniform models can be used to approximate the expected range of different embankment displacement measures, but cannot capture the complexity of the deformation mechanisms that develop in spatially variable deposits.

The Student T and the χ^2 distributions were used to assess whether additional realizations would change the distributions of representative percentiles for both single motions and for all motions (Johnson and Bhattacharyya 2011). For the smaller NSF_x values, the

distribution of representative percentiles is within a tighter distribution and therefore, additional realizations would not significantly change this distribution. For the larger NSF_x values, additional cases would improve confidence in the distributions, but the implication of the results would not change. The representative percentiles for the largest NSF_x already include cases that fall below the 10^{th} percentiles and therefore, the choice of representative percentiles for a risk or deterministic (conservative) evaluation would need to include a branch/case controlled by these lower percentiles.

CONCLUSIONS

This paper examined the selection of representative properties for use in NDAs of embankment dams of different sizes founded on a spatially variable deposit of liquefiable alluvium. NDAs were performed for models with uniform and stochastic alluvial layer properties, and the results used to determine the representative percentiles from the stochastic $(N_1)_{60cs}$ values that, when used in a uniform model, produced equal embankment displacements.

For the largest embankment (45 m high), the deformation mechanisms were large compared to the scale over which soil properties varied ($\theta_x = 20$ m) and thus there was greater averaging of soil behaviors. The representative percentiles for these models ranged from the 40^{th} to 70^{th} percentile for the set of conditions and cases examined.

For the smaller embankments (e.g., 5 or 10 m high), the deformation mechanisms were small compared to the scales over which soil properties varied (also $\theta_x = 20$ m) and thus displacements were more strongly affected by local variations in properties. The representative percentiles had much greater dispersion (or ranges) than for the 45 m high embankment, and often had values smaller than the 20^{th} percentile for the set of conditions and cases examined.

The selection of representative percentiles for use in a risk analysis will depend on the extent and location of site explorations, the geometry of the structure and deformation mechanism, the variability of soil properties and the variability of input motions among other factors. Further studies building on the results presented herein are needed to provide improved guidance on the selection of representative properties for use in deterministic or probabilistic NDA studies.

ACKNOWLEDGEMENTS

The work described herein progressed under projects for the California Division of Safety of Dams under Contract 4600009523, the Department of Water Resources under Contract 4600009751, and the National Science Foundation under grant CMMI-1635398. Any opinions, findings, conclusions, or recommendations expressed herein are those of the authors and do not necessarily represent the views of these organizations. The authors appreciate the above for their support and assistance.

REFERENCES

Ancheta, T. D., Darragh, R. B., Stewart, J. P., Seyhan, E., Silva, W. J., Chiou, B. S. J., et al. (2014). NGA-West2 database. Earthquake Spectra EERI 2014; 30(3):989-1005.

Baecher, G. B., and Christian, J. T. (2003). Reliability and statistics in geotechnical engineering, Wiley, Chichester, U.K., 619.

Boulanger, R. W., and Beaty M. H., (2016). "Seismic Deformation Analyses of Embankment Dams: A Reviewer's Checklist", In Proc., 36th USSD Annual Meeting and Conference, United States Society on Dams, 2016. 535-546.

Boulanger, R. W., and Idriss, I. M. (2012). "Probabilistic SPT-based liquefaction triggering procedure." Journal of Geotechnical and Geoenvironmental Engineering, ASCE, 138(10), 1185-1195.

Boulanger, R. W., and Montgomery, J. (2016). "Nonlinear deformation analyses of an embankment dam on a spatially variable liquefiable deposit." Soil Dynamics and Earthquake Engineering, 91, 222–233.

Boulanger, R. W., and Ziotopoulou, K. (2018). "PM4Sand (Version 3.1): A sand plasticity model for earthquake engineering applications", rep. No. UCD/CGM-17/01, Center for Geotechnical Modeling, Dept. of Civil and Environmental Engineering, Univ. of California, Davis, CA.

Duncan, J. M., and Wright, S. G. (2005). Soil strength and slope stability. J. Wiley & Sons, Hoboken.

Fenton, G. A. and Griffiths, D. V. (2005). "Three-Dimensional Probabilistic Foundation Settlement". Journal of Geotechnical and Geoenvironmental Engineering, ASCE 131(2): 232-239.

Itasca (2016). Fast Lagrangian Analysis of Continua (FLAC), release 8.0. Itasca Consulting Group, Inc., Minneapolis, MN.

Johnson, R. A., and Bhattacharyya, G. K. (2011). Statistics principles and methods. John Wiley, New York.

Mejia, K. H., and Dawson, E. M. (2006). "4th International Symposium on Numerical Modeling in Geomechanics." Minneapolis, MN.

Montgomery, J., Boulanger, R. W., Armstrong, R. J., and Malvick, E. J. (2014). "Anisotropic Undrained Shear Strength Parameters for Nonlinear Deformation Analyses of Embankment Dams." Geo-Congress 2014 Technical Papers.

Montgomery, J., and Boulanger, R. W. (2017). "Effects of Spatial Variability on Liquefaction-Induced Settlement and Lateral Spreading." Journal of Geotechnical and Geoenvironmental Engineering, 143(1), 04016086.

Perlea, V. G., and Beaty, M. H. (2010) "Corps of Engineers practice in the evaluation of seismic deformation of embankment dams." In Proceedings of the fifth international conference on recent advances in geotechnical earthquake engineering and soil dynamics. San Diego, CA.

Phoon, K.-K., and Kulhawy, F. H. (1999). "Characterization of geotechnical variability." Canadian Geotechnical Journal, 36(4), 612–624.

Popescu, R., Prevost, J. H., and Deodatis, G. (1997). "Effects of spatial variability on soil liquefaction: some design recommendations." Géotechnique, 47(5), 1019–1036.

Popescu, R., Prevost, J. H., and Deodatis, G. (2005). "3D effects in seismic liquefaction of stochastically variable soil deposits." Géotechnique, 55(1), 21–31.

Vanmarcke, E. (2010). Random fields: analysis and synthesis. World Scientific, Hackensack, NJ.